ELSEVIER

Computers and Electronics in Agriculture
34 (2002) 207–221

Computers and electronics in agriculture

www.elsevier.com/locate/compag

Numerical simulation of the airflow and temperature distribution in a tunnel greenhouse equipped with insect-proof screen in the openings

T. Bartzanas [a], T. Boulard [b], C. Kittas [a,*]

[a] *School of Agriculture Crop and Animal Production, University of Thessaly, Fytokou St., 38446 N. Ionia, Magnisias, Greece*

[b] *I.N.R.A Avignon, Unite PSH, Site Agroparc, 84914 Avignon Cedex 9, France*

Abstract

An analysis of the ventilation process in a tunnel greenhouse equipped with an insect-proof screen in the side openings was performed with the use of a commercial computational fluid dynamics (CFD) package (CFD2000®). The aim of the study was to investigate how the screen influences airflow and temperature patterns inside the greenhouse. The screens on the greenhouse inlets and outlets, as well as the crop were simulated using the porous medium approach. The first simulations were carried out with a wind direction perpendicular to the side openings. Insect screens significantly reduced airflow and increased thermal gradients inside the greenhouse. Maximum air velocity values inside the greenhouse were observed near the openings, whereas air velocity was lowest in the middle of greenhouse. Airflow rates reduced by half in the greenhouse equipped with screen. These differences were also important in the region covered by crop, thus screen affected the sensible and latent exchanges between crop and air. The effect of different wind directions was also investigated. Wind direction considerably affected climatic conditions inside the greenhouse, as contrasted air flow and temperature patterns were observed for various wind regimes, especially when the greenhouse was equipped with insect screens.

Keywords: Insect screen; Computational fluid dynamics; Airflow; Temperature distribution; Ventilation

* Corresponding author.
E-mail address: ckittas@uth.gr (C. Kittas).

0168-1699/02/$ - see front matter
PII: S0168-1699(01)00188-0

1. Introduction

Natural ventilation is considered one of the most important factors of greenhouse environment, since it directly affects transport of sensible, latent heat and CO_2 concentration to or from the interior air. In the Mediterranean area (high radiative loads) an efficient climatization is crucial in order to decrease the inside air temperature and to remove excess humidity (Boulard and Baille, 1993). Recently, many growers, in order to prevent insect intrusion and to decrease use of chemical insecticides, have adopted the use of insect proof screens on ventilation openings. Since screens provide an extra resistance to mass, momentum and heat transport and affect greenhouse microclimate, studies on airflow through screens became a topic of major importance.

Several studies were initiated to analyze the influence of insect-screens on natural ventilation. Miguel et al. (1997) used the porous media flow approach to characterize airflow flow through screens versus their aerodynamic properties, e.g. permeability and inertial factors. Other authors considered the discharge coefficient to evaluate the influence of screens on greenhouse natural ventilation (Sase and Christianson 1990; Kosmos et al., 1993). Montero et al. (1996) investigated the influence of three different screens on ventilation rates and the corresponding discharge coefficients, which were reduced up to 50%. Munoz et al. (1999) found that screens reduced overall air exchange rates and wind effect coefficient. One of the conclusions obtained from the above studies was that available greenhouse types do not provide enough air exchange when they incorporate insect-proof screens. A better understanding of the influence of screen on the ventilation process would be valuable to improve ventilation opening design in order to achieve a well-ventilated greenhouse.

None of the above studies provided details of internal flow patterns and temperature profiles. Recent progress in flow modeling by means of computational fluid dynamics (CFD) software facilitates the analysis of such scalar and vector fields by solving numerically transport equations. The first CFD simulations were carried out by Okushima et al. (1989), who compared their numerical results with the wind tunnel results of Sase et al. (1984). Even though their results agreed weakly, due to model limitations to accurately describe the grid, they obtained important information on flow patterns inside the greenhouse. In recent years CFD software has improved significantly. Among others CFD codes were used in closed greenhouses (Boulard et al., 1997a; Lamrani, 1997) and ventilated greenhouses (Mistriotis et al., 1997a,b; Boulard et al., 1999).

In the present work a commercial CFD package (CFD2000®) was used to analyze the influence of an insect-proof screen on air and temperature patterns inside the greenhouse. The analysis of the ventilation process could lead to further improvement in vent design in order to improve greenhouse climate control.

2. Theory

2.1. Flow through a porous medium

The application of Darcy's law is the standard approach to characterize single phase fluid flow in homogeneous porous media. Basically, one simply assumes that a global index, permeability K, relates the average fluid velocity u through the pores with the pressure drop ΔP measured across the system as follows:

$$u = -\frac{K}{\mu}\frac{\partial p}{\partial x} \tag{1}$$

In a three dimensional (3-D) system Eq. (1) generalizes to:

$$v = -\mu^{-1} K \nabla P \tag{2}$$

Eq. (1) is for an isothermal fluid, moving with a slow steady velocity under the action of the pressure gradient. In Eq. (1), μ is the dynamic viscosity (kg s^{-1} m^{-1}), p the pressure (Pa), x the direction of the flow (m) and K the permeability (m^2).

In spite of its great applicability, the concept of permeability as a global index for flow, which implies the validity of Eq. (1) should be restricted for Reynolds numbers ($Re = \rho u K^{0.5}/\mu$) smaller than unity as for larger Re numbers it has experimentally demonstrated the existence of a nonlinear flow regime. This motivated Forchheimer (1901) to add an extra squared fluid velocity term in Darcy's equation and Eq. (1) took the following form:

$$\frac{\partial p}{\partial x} = \frac{K}{\mu}u + \rho\left(\frac{Y}{\sqrt{K}}\right)u^2 \tag{3}$$

where ρ (kg m^{-3}) is the fluid density and Y the inertial factor (dimensionless).

Eq. (3) shows how fluid velocity is related to pressure drop, through the viscous resistance force, which appears due to momentum transfer at the fluid interface (μ/K) and the pore inertia effects ($\rho Y/K^{0.5}$).

2.2. The numerical approach

The CFD method allows the explicit calculation of the average velocity vector field of a flow by numerically solving the corresponding transport equations. The 3-D conservation equations describing the transport phenomena for steady flows in free convection are of the general form:

$$\frac{\partial(U\Phi)}{\partial x} + \frac{\partial(V\Phi)}{\partial y} + \frac{\partial(W\Phi)}{\partial z} = \Gamma\nabla^2\Phi + S_\Phi \tag{4}$$

In Eq. (4), Φ represents the concentration of the transport quantity in a dimensionless form, namely the three momentum conservation equations (the Navier–Stokes equations) and the scalars mass and energy conservation equations. U, V and W are the components of velocity vector, Γ is the diffusion coefficient and S_Φ is the source term. The governing equations are discretized following the

procedure described by Patankar (1980). This consists of integrating the governing equations over a control volume.

The software used for the simulations, uses a finite-volume discretization code, the pressure implicit with splitting of operators (PISO) algorithm developed by Issa (1985), to solve the set of equations describing the transport phenomena. A standard $k-\varepsilon$ model (Launder and Spalding, 1974) assuming isotropic turbulence was adopted to describe turbulent transport. This choice is a good compromise for a realistic description of turbulence and computational efficiency (Jones and Whittle, 1992). The complete set of the equations of the $k-\varepsilon$ model can be found in Mohammadi and Pironneau (1994) and their commonly used set of parameters (empirically determined) are given in CFD 2000 (1998). For the geometry a control volume was selected representing a large domain (38 m long, 50 m wide and 20 m high) including the greenhouse (Fig. 1a). The computational grid of the CFD software used Cartesian coordinates and a finer resolution was imposed in critical portions of the flow subject to strong gradients (Fig. 1b). Body-fitted coordinates were also applied to exactly conform the grid to the contours of the boundary conditions. The boundary conditions prescribed a null pressure gradient in the air, at the limits of the computational domain, and wall-type boundary conditions along the floor and the roof whereas the side walls were treated as adiabatic. The selected boundary conditions as well as the dimensional parameters of the greenhouse structure used in the simulations are given in Table 1. The outside air speed was $u = 2$ m s^{-1} perpendicular to the openings. The driving force of natural convection is the wind force and the buoyancy force arising from small temperature differences within the flow according to the Boussinesq hypothesis. The insect screen was simulated as porous medium. The values of the aerodynamic properties of the porous medium (screen) used as boundary conditions were calculated using relations from the literature, which correlate these properties (permeability and inertial factors) with the porosity (Miguel et al., 1997). Thus the permeability and the inertial factors of the screen were calculated according to the following equations (Miguel et al., 1997):

$$K = 3.44 \times 10^{-9} \varepsilon^{1.6} \tag{5}$$

$$Y = 4.30 \times 10^{-2} \varepsilon^{2.13} \tag{6}$$

where ε is screen porosity.

Screen porosity can be determined by magnifying one sample with a microscope and by measuring the area filled with air and the area occupied by solid matrix and air.

The crop was simulated using the porous medium approach. Crop aerodynamic properties were determined in a similar way with the screen. For reasons of simplicity we assumed that pressure forces contributed to the major portion of total canopy drag (Thom, 1971). The form drag appearing in the source terms of momentum equations was modeled as:

$$\frac{\partial P}{\partial X} = C_{\mathrm{D}} \mathrm{LAI} \rho u^2 \tag{7}$$

where LAI is the crop leaf area index and C_D is the canopy drag coefficient.

From Eqs. (3) and (7) we can deduce that:

$$Y = C_D \mathrm{LAI} K^{0.5} \tag{8}$$

From Eq. (8) it is obvious that crop aerodynamic characteristics can be determined if we know the pressure drop across the crop. For a well-developed tomato

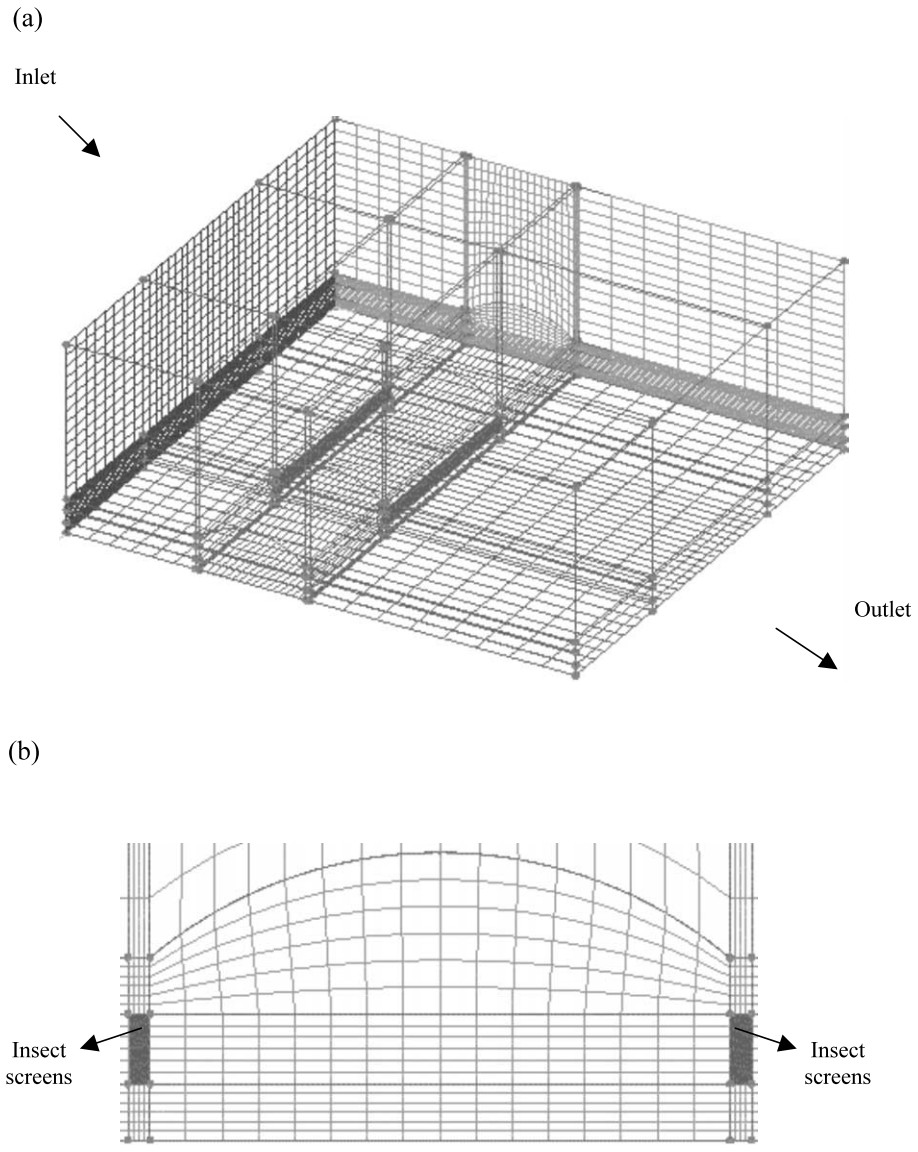

Fig. 1. Computational grid of the whole domain (a) and detailed grid of the greenhouse region (b).

Table 1
Boundary values and greenhouse dimensions used in the simulations

Parameters	Numerical value	Dimensions
Heat transfer through greenhouse floor	228	W m^{-2}
Heat transfer through greenhouse sides	Adiabatic	
Heat transfer through greenhouse roof	30	W m^{-2}
Outside air temperature	300	K
Outside wind speed	2	m s^{-1}
Outside soil temperature	303	K
Crop permeability	0.395	m^2
Crop non-linear loss coefficient	0.2	Dimensionless
Insects screens permeability	2×10^{-6}	m^2
Insects screens non-linear loss coefficient	0.01	Dimensionless
Greenhouse length	8	m
Greenhouse width	20	m
Side height	2.5	m
Ridge height	4.1	m
Vent opening	0.9	m
Crop height	1.2	m

crop (LAI = 4), $C_D = 0.2$, the corresponding values for permeability and non-linear loss coefficient are $K = 0.395$ and $Y = 0.2$ (Haxaire, 1999).

3. Results and discussion

3.1. Influence of the screen on airflow and temperature distribution

As expected, screen incorporation onto the greenhouse openings significantly affected air flow and temperature distribution inside the greenhouse. Fig. 2 presents the velocity vectors for the two cases (without and with screen) in a vertical plane at the middle of the greenhouse. For the greenhouse without screen (Fig. 2a), internal airflow was characterized by a strong flow near the greenhouse floor and a slow circulation near the roof and a counter flowing current with respect to outside wind. Most of the air leaves the greenhouse volume without good mixing. For the greenhouse with screen (Fig. 2b) a similar airflow pattern was observed, with lower values for velocity but better air mixing in the internal space. Thus, for the examined case (shape and position of the openings) better air mixing was achieved in the greenhouse with screen.

The temperature pattern follows airflow distribution. Fig. 3 presents the temperature distribution in a horizontal plane 0.6 m from the ground. A thermal gradient was observed for the two cases especially at the regions where the velocity magnitude of the internal air had small values. It is clear that this heterogeneity was more important for the greenhouse with screen (Fig. 3b). The maximum temperature difference, with respect to the outside temperature, was 3 °C for the green-

house without screen (Fig. 3a) whereas for the greenhouse with screen (Fig. 3b) this difference was increased up to 7 °C.

Air velocity inside the greenhouse had maximum values near the openings ($x = 0$ m), whereas in the middle of the greenhouse ($x = 4$ m) air velocity was small (Fig. 4). Negative values were due to counter flow with respect to outside wind direction. Where there was no screen in the openings the inside air temperature was almost equal to the outside (300 K) (Fig. 5). The use of a screen resulted in a gradual temperature increase inside the greenhouse. The air entered the greenhouse ($x = 0$ m) with a temperature similar to the outside one and left ($x = 8$ m) 4 °C warmer. We must remark that temperature elevation can be even greater at other places inside the greenhouse.

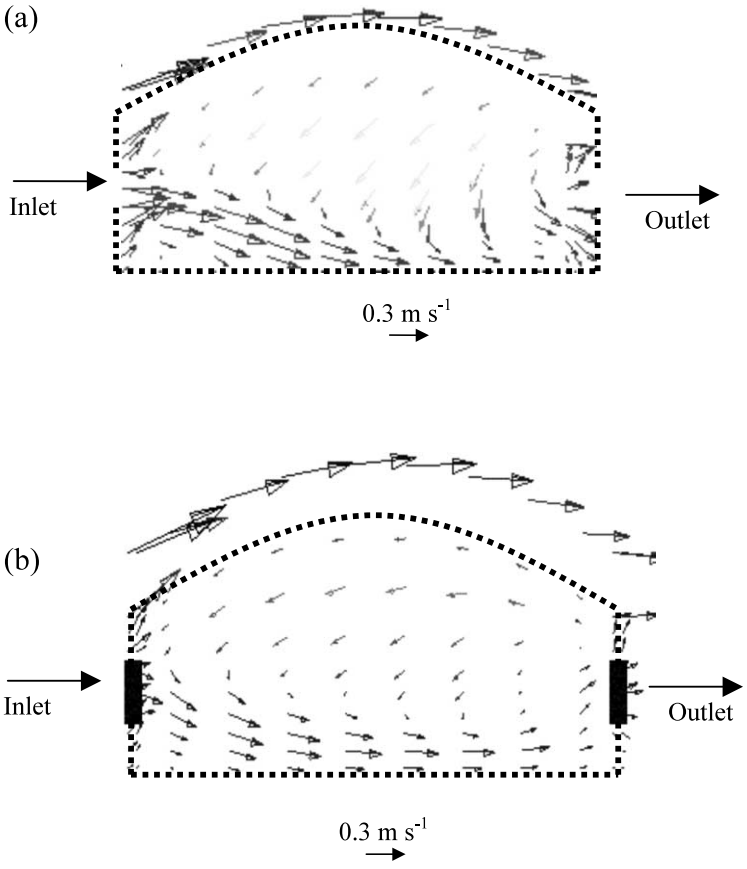

Fig. 2. Velocity vectors in a vertical plane at the middle of greenhouse. (a) Greenhouse without screen; (b) greenhouse with screen.

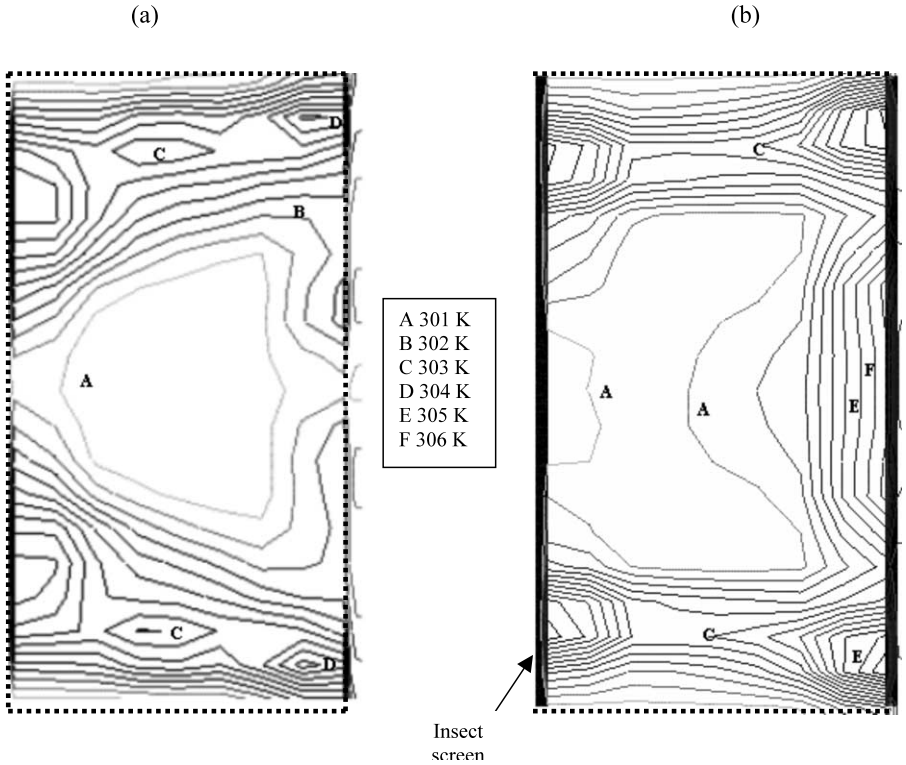

Fig. 3. Influence of the screen in air temperature distribution in a horizontal plane 0.6 m from the ground. (a) Greenhouse without screen; (b) greenhouse with screen.

3.2. Influence of the screen on the airflow rates

Integrating air speed, as developed above, over a complete cross-section of the greenhouse opening allows for estimation of airflow rate G, as follows:

$$G = L\int_0^H u_y \mathrm{d}y \tag{9}$$

where G ($m^3\ s^{-1}$) is the airflow rate, u_y ($m\ s^{-1}$) is the vertical component of air velocity through the opening, L (m) and H (m) are the opening length and height, respectively.

For both cases (greenhouse with or without screen), airflow rate was estimated according to Eq. (9). For the greenhouse with screen, airflow rate was estimated as $G = 1.7\ m^3\ s^{-1}$ which allows 20 air renewals per hour. This value is very low. For the greenhouse without screen the estimated ventilation rate was $G = 3.8\ m^3\ s^{-1}$ which allows 45 air renewals per hour. Consequently, the use of screen on ventilation openings reduces airflow rates by half.

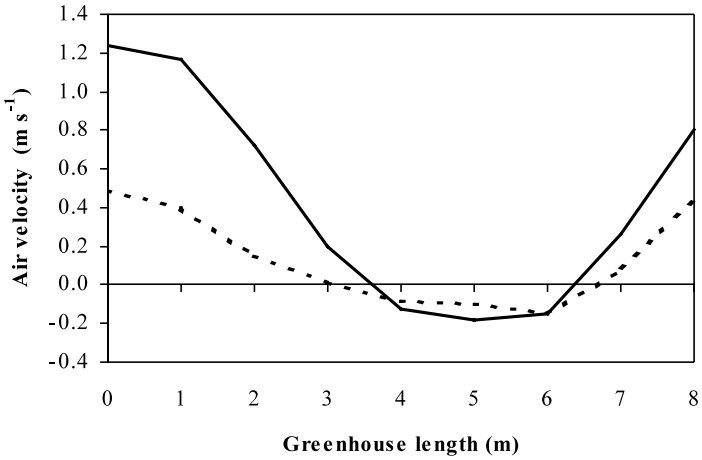

Fig. 4. Air velocity distribution along the greenhouse at the middle of the openings. Greenhouse without screen (——), greenhouse with screen (----).

3.3. Air flow and temperature distribution in the crop region

Maintaining uniform climatic conditions in the region occupied by the crop is one of the major goals of greenhouse climate management. Air velocity near the leaves affects boundary layer resistance and thus, the fluxes of energy, water vapor and CO_2 between leaves and the surrounding air. As it was reported by Fernandez and Bailey (1994), the crop results in an irregular distribution of air movement in greenhouses, with areas remaining unaffected by the airflow, and areas being under high air velocities. Fig. 6 presents the influence of screen on air velocity distribution along the greenhouse at the middle of the crop (0.6 m from greenhouse floor). The

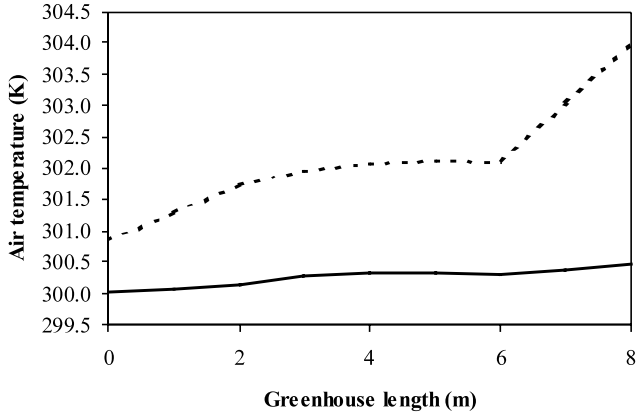

Fig. 5. Air temperature distribution along the greenhouse at the middle of the openings. Greenhouse without screen (——), greenhouse with screen (----).

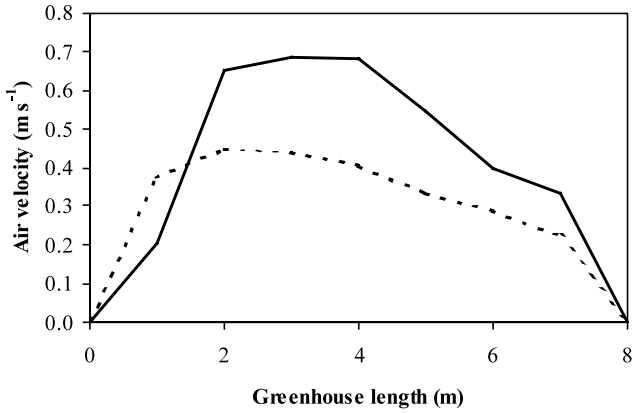

Fig. 6. Air velocity distribution along the greenhouse in the middle of the crop (0.6 m from greenhouse floor). Greenhouse without screen (——), greenhouse with screen (----).

screen reduced air velocity from 0.7 (at the middle of the greenhouse $x = 4$ m) to 0.35 m s^{-1}. This air velocity decrease resulted from boundary layer resistance and, consequently, a decrease in the convective heat transfer coefficient. The influence of screen on air temperature distribution along the greenhouse (in the middle of the crop) is presented in Fig. 7. A strong thermal gradient occurs, especially in the leeward section of the greenhouse ($x = 8$ m). In this section, temperature difference between the two greenhouses (with and without screen) reached about 3.5 °C.

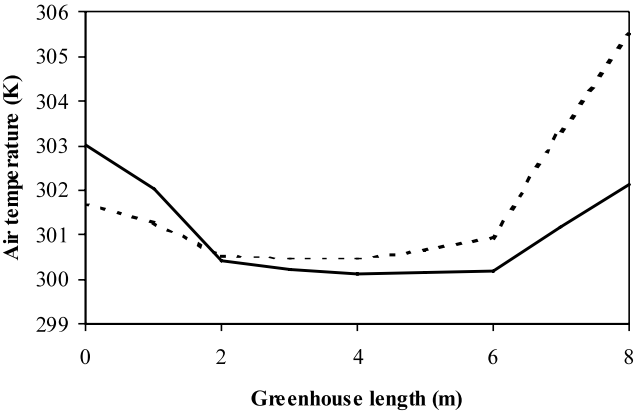

Fig. 7. Air temperature distribution along the greenhouse in the middle of the crop (0.6 m from greenhouse floor). Greenhouse without screen (——), greenhouse with screen (----).

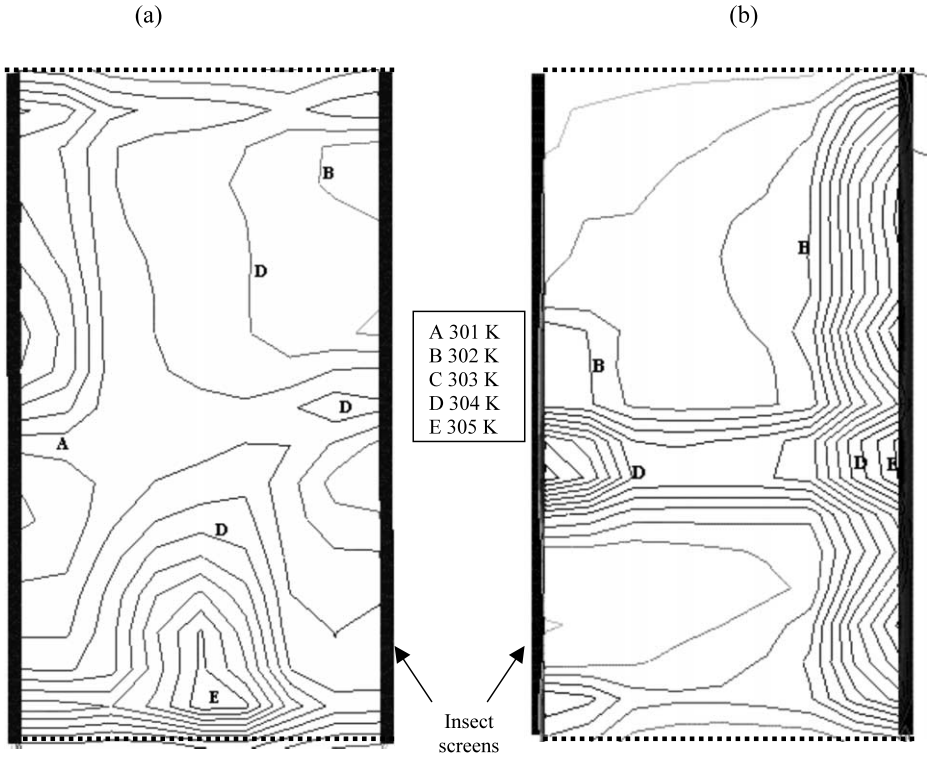

Fig. 8. Influence of wind direction on air temperature distribution, in a horizontal plane in the middle of the crop (0.6 m from greenhouse floor), in the screened greenhouse. (a) Wind direction parallel to the openings; (b) wind direction with 45° to the openings.

3.4. Influence of wind direction on airflow and temperature distribution inside the greenhouse

In the literature, the analysis of the effect of wind direction on ventilation rate is not very clear. Some authors (Bot, 1983) found important effects while others (Fernandez and Bailey, 1992) did not find significant changes with direction. The influence of wind direction on airflow was examined numerically for two cases for the screened greenhouse, a wind parallel to the opening areas; and a wind blowing with a 45° angle with respect to the opening areas. Fig. 8 presents the temperature distribution in an horizontal plane situated 0.5 m from the ground. For both cases, distribution of temperature inside the greenhouse was quite different and the resultant temperature profile was mainly affected by airflow. When the wind was parallel to the openings (Fig. 8a), both openings acted simultaneously as inlets and outlets. Air entered the greenhouse through the leeward section of the openings and exited through the windward part and, consequently the windward end of the greenhouse was always warmer. Similar airflow pattern was measured in a green-

house with a continuous roof (Boulard et al., 1997b). This phenomenon is similar to the so-call 'side wall effect' observed Fernandez and Bailey (1992) from tracer gas measurements. The windward gable end induced a static pressure field with a relative contribution to the whole ventilation rate inverse to the size of the greenhouse. When the air flow was at an angle of 45° with respect to the openings (Fig. 8b), the air entered through the windward opening but with a lower intensity. Consequently, the leeside section was warmer. Fig. 9 illustrates the different airflow patterns at the level of the openings in a horizontal plane for the two wind directions (Fig. 9a, wind parallel to the openings; and Fig. 9b, wind 45° with openings). Air velocity distribution along the greenhouse, at the middle of the openings, is presented in Fig. 10, whereas the corresponding air temperature

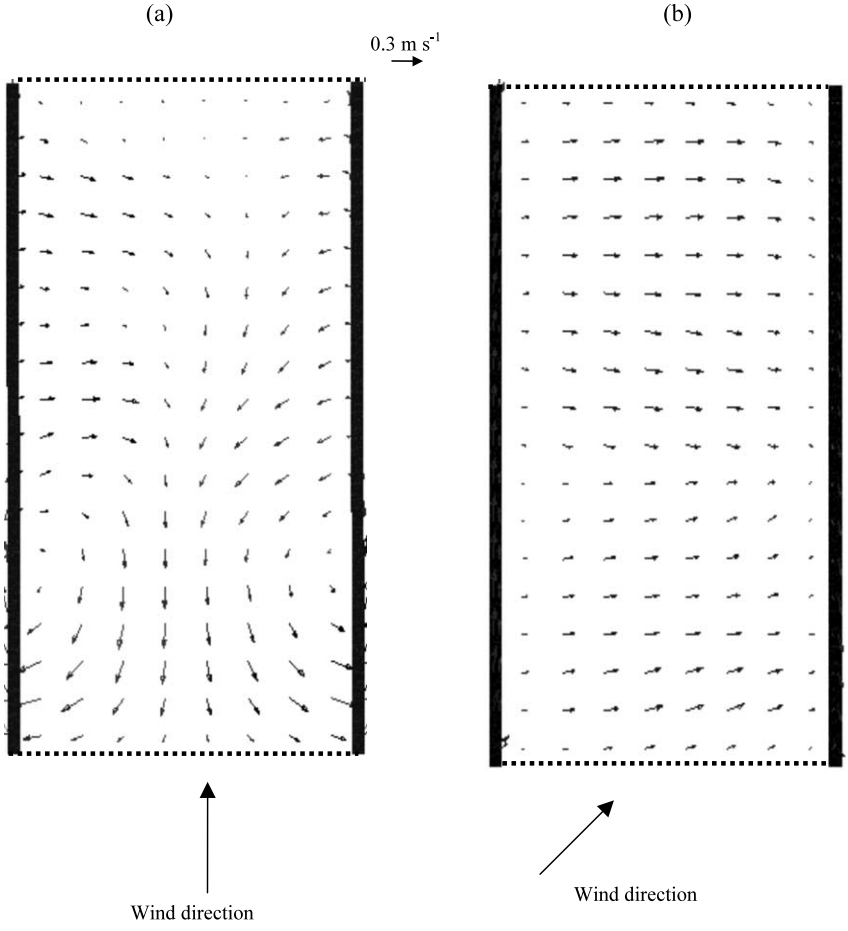

Fig. 9. Influence of wind direction on air velocity distribution, in a horizontal plane in the middle of the openings, in the screened greenhouse. (a) Wind direction parallel to the openings; (b) wind direction with 45° to openings.

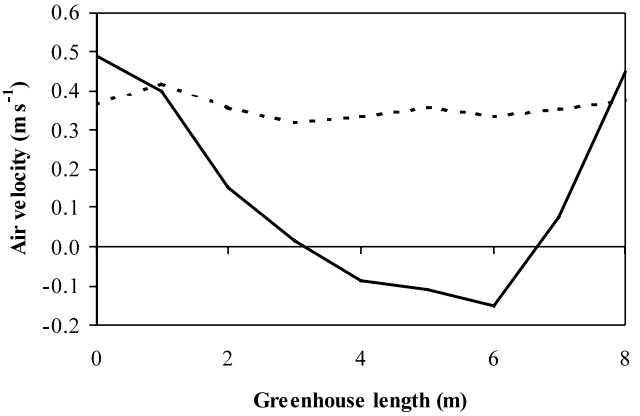

Fig. 10. Influence of wind direction on air velocity distribution along the screened greenhouse, in the middle of the openings. Wind direction parallel to the openings (——), wind direction with 45° to the openings (----).

distribution (in the middle of the openings) is presented in Fig. 11. When outside air flew with 45° in respect to the openings, both air velocity and temperature had a uniform distribution along the greenhouse and air velocity varied between 0.3 and 0.4 m s^{-1}. When air flow was parallel to the openings and each opening acted as an inlet and an outlet, we observed regions inside the greenhouse, mainly in the middle of greenhouse, with very low air velocities (0.05–0.1 m s^{-1}). Consequently, temperature gradually increased between the two openings up to 5 °C higher than the outside air.

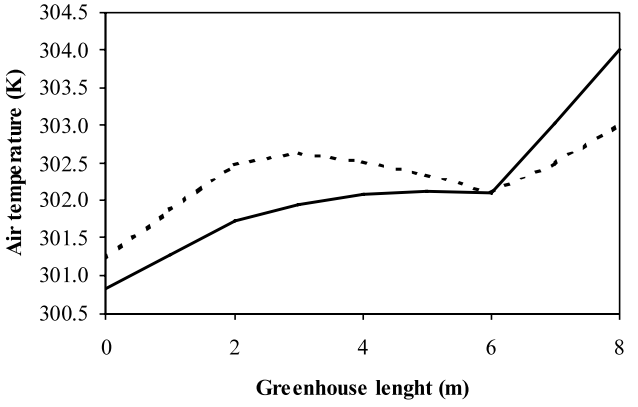

Fig. 11. Influence of wind direction on air temperature distribution along the screened greenhouse, in the middle of the openings. Wind direction parallel to the openings (——), wind direction with 45° to the openings (----).

4. Conclusions

The influence of an insect proof screen on airflow and temperature patterns was numerically investigated for a tunnel greenhouse with continuous side openings by means of a CFD package. The simulation results indicated that the screen had a considerable effect on greenhouse climate. A screen strongly reduced air velocity inside the greenhouse (especially inside the crop area) and airflow rate (50% reduction) resulting in a significant temperature increase. With respect to outside temperature (27 °C), maximum temperature augmentation was 3 °C higher for the greenhouse without screen and up to 7 °C higher for the greenhouse with screen. The crop acted as extra resistance to airflow and modified airflow and temperature distribution. Wind direction also affected airflow and temperature distribution inside the greenhouse (contrasted airflow and temperature patterns were observed for various wind regimes) and this must be considered especially in greenhouses equipped with insect screens. These results concern only the specific case examined. Therefore, the conclusions, although they give a good qualitative picture on the influence of screens, can hardly be generalized.

References

Bot, G.P.A., 1983. Greenhouse climate: from physical processes to a dynamic model. Ph.D. Thesis, Agricultural University of Wageningen.

Boulard, T., Baille, A., 1993. A simple greenhouse climate control model incorporating effects of aeration and evaporative cooling. Agric. For. Meteorol. 65, 145–157.

Boulard, T., Roy, J.C., Lamrani, M.A., Haxaire, R., 1997a. Characterising and modelling the air flow and temperatures profiles in a closed greenhouse in diurnal conditions. Mathematical and Control Applications in Agriculture and Horticulture; IFAC Workshop; Hanover, Germany.

Boulard, T., Papadakis, G., Kittas, C., Mermier, M., 1997b. Air flow and associated sensible heat exchanges in a naturally ventilated greenhouse. Agric. For. Meteorol. 88, 111–119.

Boulard, T., Haxaire, R., Lamrani, M.A., Roy, J.C., Jaffrin, A., 1999. Characterization and modelling of the air fluxes induced by natural ventilation in a greenhouse. J. Agric. Eng. Res. 74, 135–144.

CFD2000/STORM v.3.0, 1998. Computational Fluid Dynamics systems, Pacific Sierra Corp., USA.

Fernandez, J.E., Bailey, B.J., 1992. Measurements and prediction of greenhouse ventilation rates. Agric. For. Meteorol. 58, 229–245.

Fernandez, J.E., Bailey, B.J., 1994. The influence of fans on environmental conditions in greenhouses. J. Agric. Eng. Res. 58, 201–210.

Forchheimer, P., 1901. Wasserbewegung durch boden. Z. Ver. Deutsch. 45, 1782–1788.

Haxaire, R., 1999. Caracterisation et modelisation des ecoulements d'air dans une serre. Ph.D. Thesis, University of Nice Sophia Antipolis, France.

Issa, R.I., 1985. Solution of the implicity discretised fluid flow equations by operator. J. Comput. Phys. 62, 40–54.

Jones, P.J., Whittle, G.E., 1992. Computational fluid dynamics for building airflow prediction. Build. Env. 27, 321–338.

Kosmos, S.R., Riskowski, G.L., Cristianson, L.L., 1993. Force and static pressure resulting from airflow through screens. Trans. ASAE 36, 1467–1472.

Lamrani, M.A., 1997. Characterization and modeling of the natural laminar and turbulent convection in a greenhouse. Ph.D. thesis, University of Agadir, Morocco.

Launder, B.E., Spalding, D.B., 1974. The numerical computation of turbulent flows. Comp. Meth. App. Mech. Eng. 3, 269–289.

Miguel, A.F., van de Braak, N.J., Bot, G.P.A., 1997. Analysis of the airflow characteristics of greenhouse screening materials. J. Agric. Eng. Res. 67, 105–112.

Mistriotis, A., Arcidianoco, C., Picuno, P., Bot, G.P.A., Scarascia Mugnozza, G., 1997a. Computational analysis of the natural ventilation in greenhouses at low wind speed. Agric. For. Meteorol. 88, 121–135.

Mistriotis, A., Bot, G.P.A., Picuno, P., Scarascia Mugnozza, G., 1997b. Analysis of the efficiency of greenhouse ventilation with computational fluid dynamics. Agric. For. Meteorol. 85, 317–328.

Mohammadi, B., Pironneau, O., 1994. Analysis pf the k–epsilon turbulence model. In: Research in Applied Mathematics. Wiley, New York/Masson.

Montero, J.I., Munoz, P., Anton, A., 1996. Discharge coefficients of greenhouse windows with insect-proof screens. Acta Hortic. 443, 71–77.

Munoz, P., Montero, J.I., Anton, A., Giuffrida, F., 1999. Effect of insect-proof screens and roof openings on greenhouse ventilation. J. Agric. Eng. Res. 73, 171–178.

Okushima, L., Sase, S., Nara, M., 1989. A support system for natural ventilation design of greenhouses based on computational aerodynamics. Acta Hortic. 248, 129–136.

Patankar, S.V., 1980. Numerical Heat Transfer. Hemisphere, Washington.

Sase, S., Christianson, L., 1990. Screening greenhouse—some engineering considerations. ASAE Paper No. NABEC, 90–201.

Sase, S., Takakura, T., Nara, M., 1984. Wind tunnel testing on airflow and temperature distribution of a naturally ventilated greenhouse. Acta Hortic. 148, 329–336.

Thom, A.S., 1971. Momentum absorption by vegetation. Quart. J. R. Meteorol. 97, 414–428.